

Rapid detection of dengue virus in serum using magnetic separation and fluorescence detection

Won-Suk Chang,^{†a} Hao Shang,^{†a} Rushika M. Perera,^b Shee-mei Lok,^b Dagmar Sedlak,^b Richard J. Kuhn^b and Gil U Lee^{*a}

Received 18th July 2007, Accepted 30th November 2007

First published as an Advance Article on the web 20th December 2007

DOI: 10.1039/b710997k

A magnetophoretic fluorescence sensor (MFS) has been developed to rapidly detect dengue virus in serum at a sensitivity that was approximately three orders of magnitude higher than conventional solid phase immunoassays. UV inactivated type 2 dengue virus was first reacted with a mixture of superparamagnetic and fluorescent microparticles functionalised with an anti-type 2 dengue virus monoclonal antibody in 10% fetal calf serum. The magnetic particles were separated from the serum based on their magnetophoretic mobility, and dengue virus was detected by the co-localization of magnetic and fluorescent particles at a specific point in the flow chamber. The MFS was capable of detecting dengue-2 virus at 10 PFU ml⁻¹ with a reaction time of 15 min. The MFS demonstrated a high specificity in the presence of yellow fever virus, a closely related flavivirus, which also did not produce any detectable increase in background signal. The improved performance of this technique appears to result from the rapid kinetics of the microparticle reaction, improved signal-to-noise ratio resulting from magnetophoretic separation, and rapid fluorescent particle detection. These results suggest that the MFS may be useful in early stage diagnosis of dengue infections, as well as other diseases.

Introduction

It is becoming increasingly clear that the global community is vulnerable to the rapid spread of infectious diseases, as we have seen several viruses mutate, jump between species, and spread through our integrated economy.^{1–3} Early stage detection in patients could enhance recovery and also limit the spread of the disease. Therefore, there is a particular need for rapid, sensitive, and inexpensive point-of-care sensors that are capable of simultaneously identifying multiple pathogens in complex samples such as blood.

The development of superparamagnetic microparticles has made it possible to rapidly and efficiently separate cells from complex mixtures, such as fermentation broths and culture media, in a manner that does not require complicated equipment.^{4,5} In this technique the magnetic particles are coated with antibodies (or other receptors) that react with specific ligands on the cells of interest and are allowed to reaction with the sample. A magnet is then used to separate the magnetic particles and the specific cell type of interest in a single step. Magnetic separation is exceptionally efficient because most biological materials are not susceptible to magnetic fields.^{6,7} It has also proven to be a very effective means of identifying specific cell lines, as demonstrated by the report that the genotype of 7–22 fetal cells has been identified in 16 ml of maternal blood.⁸

Magnetophoresis is a separation process in which both hydrodynamic and magnetic fields are used to separate a magnetic material from an aqueous solution on a continuous basis. In high volume, continuous industrial applications, high-gradient fields have been used to collect large quantities of magnetic material from suspensions.^{9–11} Highly efficient rare cell purification has also been achieved using high-gradient, continuous magnetic separation.^{12,13} Recently, superparamagnetic microparticles have been separated in microfluidics systems using magnetophoresis.^{14,15} In such assays, the particles travel at the same velocity with the buffer in a laminar flow regime and a perpendicular magnetic field is applied to deflect the particle flow to collect the particles in different wells. By independently tuning the scale of the two forces the particles can be sorted into different regions based on their size, magnetic susceptibility, and loading of magnetic materials. Alternatively, an inductive magnetic field can be produced by a wire to direct magnetic material to a central well, whereas the non-magnetic material was separated into two side streams.¹⁶

In this report, we demonstrate magnetophoretic separation and fluorescence detection of type 2 dengue virus. We chose to study dengue, a member of the flavivirus genus of enveloped RNA viruses, as it is one of the most significant mosquito-borne viral pathogens, given the impact of the recent resurgence of dengue fever and dengue hemorrhagic fever.¹⁷ There are four dengue virus serotypes namely dengue 1, 2, 3, and 4. Severe dengue hemorrhagic fever can develop in children and adults experiencing a second dengue virus infection with a serotype different from that of their first dengue virus infection. Currently, dengue is identified using immunocolorimetric assays that detect the immunoglobulin M

^aSchools of Chemical and Biomedical Engineering, Forney Hall, Purdue University, West Lafayette, IN 47907, USA. E-mail: gl@ecn.purdue.edu; Tel: +1-765-494-0492

^bDepartment of Biological Sciences, Lilly Hall, Purdue University, West Lafayette, IN 47907, USA

[†] These authors contributed equally.

(IgM) or G (IgG) antibody response. This assay suffers from three limitations: an antibody is not detectable until the patient is infected for 5 days, some patients do not show IgM in the secondary infection, and they are prone to false positives, which arise from the polyclonal antibody produced by the patients infected with flavivirus viruses having similar protein structure with dengue, such as yellow fever. Development of a sensor capable of directly detecting dengue at a concentration $<10^3$ virus per ml would allow the disease to be detected at day 2, when the symptoms first become evident.

The MFS detects the virus through a series of four steps. First, magnetic and fluorescent microparticles were reacted at a concentration of approximately 10^4 particles per ml, with killed type 2 dengue virus at a concentration of $1-10^4$ PFU

m^{-1} (plaque forming unit). These particles were functionalized with monoclonal antibodies against type 2 dengue virus using a polyethylene glycol (PEG) chemistry that minimizes the non-specific adsorption of proteins from the sample.¹⁸ The product of this reaction was a mixture of a large number of individual particles and a smaller number of magnetic–fluorescent, magnetic–magnetic, and fluorescent–fluorescent particles assembled through an antibody–virus–antibody bond (Fig. 1A). Second, the magnetic particles were concentrated from the sample using a single step magnetic separation to allow the unbound fluorescent particles to be rapidly and efficiently separated from those bound to magnetic particles. Third, magnetophoresis was used to concentrate the fluorescent–magnetic particle complexes in a defined region of a

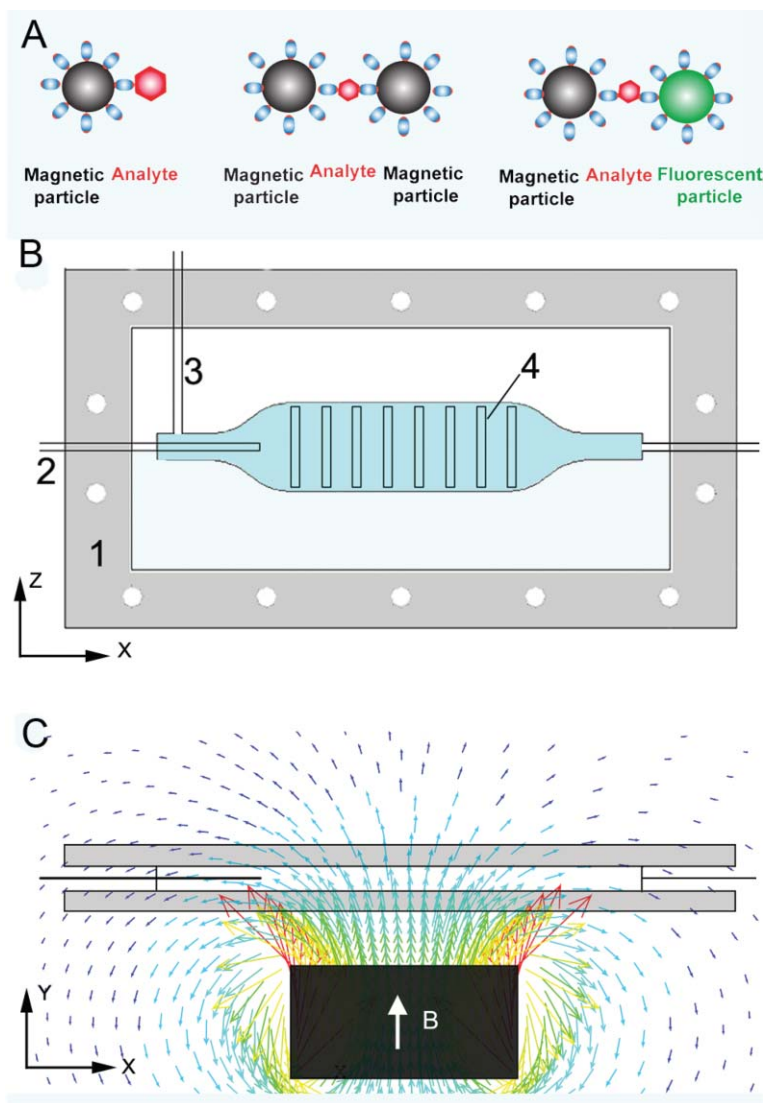


Fig. 1 (A) Schematic presentation of three assemblies that are collected by the separator. Magnetic particles that react with just virus (left) or another magnetic particle (middle) are not detected by MFS. Only magnetic–fluorescent particles assemblies (right) are detected. (B) Top view of the magnetic separator (1) in which particles with bound pathogens enter at the left of the flow chamber (2) and are transported in the x -direction by the carrier fluid (3) moving at v_h . The permanent magnet generates a magnetic field gradient that causes the particles to move primarily in the y -direction at a velocity v_m . The particles are collected and identified in the wells (4) at the surface of the flow chamber. (C) Side view of magnetic separator with magnetic field vectors emanating from the permanent magnet. The color and length of the arrows represent the magnetic field strength as calculated using finite elements analysis.

flow cell (Fig. 1B and C) so that they could be rapidly detected with a high signal-to-noise ratio in the last step. Type 2 dengue virus was detected in 20 ml of 10% fetal calf serum at a sensitivity of 10 PFU ml^{-1} with a reaction time of 15 min, a separation time of 40 min, and a detection time of 10 min. The specificity of this assay was demonstrated by spiking the sample with yellow fever virus as a control. The high sensitivity, high specificity, and rapid response time of the MFS suggest it is a promising candidate for early identification of dengue virus in point-of-care use.

Experimental

Preparation of paramagnetic particles

The magnetic particles were prepared by the emulsion templated self-assembly technique.¹⁹ A crude oil-in-water emulsion was prepared by vortexing the nanoparticle-hexane solution with 40 mM sodium dodecyl sulfate (SDS) solution at a 1 : 4 ratio. The size of the droplet was refined by passing it through a 2 μm Isopore membrane (Millipore, Billerica, MA, USA). The emulsion was diluted at a 1 : 27 ratio in a 40 mM SDS solution and hexane was allowed to evaporate overnight at room temperature on a rotator. The particles were subsequently mixed with 10% acrylic acid in aqueous solution. Polymerization was carried out by exposing the particles to a 20 mW cm^{-2} ultraviolet light for 10 min. The particles were collected with a permanent magnet, rinsed with water three times, and stored at 4 °C. The diameter of the particle was determined by transmission electron microscopy to be $1.07 \pm 0.07 \mu\text{m}$, and their magnetization was measured with a SQUID magnetometer to be 50.6 emu g^{-1} (Quantum Design, San Diego, CA, USA).

Preparation of the viruses and antibodies

The dengue and yellow fever viruses were prepared in a BSL-2 (Biosafety level-2) environment, which is suitable for work involving agents of moderate potential hazard to personnel and environment. Dengue virus type 2, strain PR159-S1²⁰ was grown in mosquito C6/36 cells (ATCC CRL-1660, Manassas, VA, USA) adapted to minimal essential medium (Gibco/Invitrogen, Carlsbad, CA, USA).²¹ The virus titer was determined by plaque assay in baby hamster kidney cells. Yellow fever virus strain 17D was grown as described previously.²² Both dengue and yellow fever viruses were inactivated by exposure of the virus to UV light for 30 min.

The mouse anti-dengue antibody 9A3D-8 (a gift from John Roehrig, Centers for Disease Control and Prevention, Atlanta, GA, USA) was produced from hybridoma cells and purified on a protein G column (GE Healthcare, Piscataway, NJ, USA).²³ Hybridoma cells were grown in BD Cell MAb Medium in a CELLLine device (BD Bioscience, San Jose, CA, USA). Tissue culture supernatant containing antibodies were harvested over three weeks. The tissue culture supernatant was spun at $2000 g$ for 10 min and the supernatant was stored at $-20 \text{ }^\circ\text{C}$. Purification of the antibodies was carried out by first thawing the supernatant and dialyzing it in 20 mM sodium phosphate buffer, pH 7.0 overnight at 4 °C. The sample was filtered through a $0.22 \mu\text{m}$ filter membrane and then passed

through a protein G column. The antibodies were eluted using 100 mM glycine-HCl, pH 2.7. The antibodies were immediately neutralized by addition of 1 M Tris-HCl, pH 9.0 and then dialyzed in 20 mM sodium phosphate buffer, pH 7.0. Antibodies were concentrated to approximately 15 mg ml^{-1} using an Amicon Ultra concentrator (Millipore, Billerica, MA, USA).

Modification of paramagnetic and fluorescence particles with antibody

The surface of the paramagnetic particles was modified with carboxyl groups that were readily available for covalent coupling of proteins and other molecules. Magnetic particles were functionalized with the anti-dengue antibody by covalent bond attachment through a PEG monolayer, as described previously.²⁴ The particles were first coated with a monolayer of primary amines by physically adsorbing polyethylene imine (PEI, Polymin SNA, BASF, Rensseler, NY, USA) on the negatively charged particles. These surfaces were then functionalized with a vinyl-sulfone PEG monolayer by reacting α -vinyl sulfone, ω -N-hydroxysuccinimidyl ester of poly(ethylene glycol)-propionic acid (NHS-PEG-VS) (Nektar, Huntsville, AL, USA) with the PEI coated particles. The antibody was modified with sulfhydryl groups using *N*-succinimidyl-S-acetylthioacetate (SATA, Pierce Biotechnology, Rockford, IL, USA) at 1 : 10 ratio in 100 mM phosphate buffer, 150 mM NaCl, and 10 mM EDTA at pH 7.2. The sulfhydryl group was activated with a deacetylation buffer of 50 mM hydroxylamine-HCl, 2.5 mM EDTA, 62.5 mM $\text{Na}_2\text{HPO}_4\text{-NaH}_2\text{PO}_4$ at pH 7.5 for 2 h. The buffer was replaced on a cellulose desalting column (Pierce, Rockford, IL, USA) with 50 mM $\text{Na}_2\text{HPO}_4\text{-NaH}_2\text{PO}_4$, 1 mM EDTA, pH 7.2. Approximately 10^{10} PEG-VS particles were reacted with 700 μg of the SATA activated antibody in desalting buffer. The $1 \pm 0.1 \mu\text{m}$ green fluorescent micro-particles (Duke Scientific, Palo Alto, CA, USA) were modified with anti-dengue antibody by following the same procedure.

Magnetophoretic sensor design and operation

The magnetophoretic sensor design is presented in Fig. 1B. The main component of the sensor is a 20 mm wide, 110 mm long flow chamber, which was constructed from a 2 mm PDMS layer sandwiched between glass and transparent plastic plates. The flow chamber was assembled with two aluminium frames and eight collection wells were cut in the bottom plate with the dimensions of $2 \times 20 \text{ mm}$ at 5 mm interval. Two syringe pumps (not shown) were used to introduce particles and buffer using 5 and 150 ml syringes, respectively. The chamber shape in the entrance and exit regions was streamlined to avoid turbulence. A rectangular glass capillary (VitroCom, Mountain Lakes, NJ, USA) with internal dimensions of $0.05 \times 1 \text{ mm}$ was inserted at the center of the flow chamber to introduce the magnetic particles. The carrier fluid inlet and outlet were made with 1.17 mm inner diameter stainless steel tubing (Upchurch, Oak Harbor, WA, USA). The flow rates were chosen to allow well-defined laminar flow to be established at the entrance region of the magnetic particles and over the collection wells. A $50.8 \times 50.8 \times 25.4 \text{ mm}$ rare earth

neodymium iron boron (NdFeB 35, K&J Magnetics, Jamison, PA, USA) magnet was placed 16 mm under the chamber to provide a magnetic field for magnetophoretic separation. The field generated by this magnet was characterized using finite elements modelling (ANSYS, Canonsburg, PA, USA) as shown in Fig. 1C. These calculations were confirmed by measuring the magnetic flux with a Hall probe (DTM-133 digital teslameter, GMW associates, San Carlos, CA, USA) as a function of perpendicular distance from the center of the magnet. The magnetic and fluorescent particles were counted in the collection wells with an inverted optical microscope (Nikon TE300 with 40 \times ELWD lens) equipped with a 450/510 nm excitation-emission filter set, a cooled CCD camera (Coolsnap HQ, Roper Scientific, Tucson, AZ, USA) and an XYZ motorized stage (Prior, Rockland, MA, USA).

Magnetophoretic assay

The dengue viruses were detected using the fluorescent–virus–magnetic particle assay in 10% fetal bovine serum (Sigma, St. Louis, MO, USA). About 1×10^4 anti-dengue magnetic particles per millilitre and 7×10^4 anti-dengue fluorescent particles per millilitre were added to either 5 or 20 ml 10% fetal calf serum diluted into pH 7.2 phosphate buffered saline (PBS, 12 mM phosphate buffer with 150 mM NaCl) with 0.02% Tween 20. UV-inactivated dengue virus was added to this mixture at dilutions of 1, 10, 100, 1000, 10 000 PFU ml⁻¹. After incubation in a 15 or 50 ml test tube at room temperature for 15 min on a rotation wheel (Labquake, Barnstead International, Dupoque, IA, USA), the particles were separated from the solution using a block magnet in 2 min. After the first magnetic separation, the particles were redispersed in their original volume of PBS. The particle solution was fed into the flow chamber at 0.5 ml min⁻¹ with the carrier buffer flow rate at 10 ml min⁻¹. After the particle separation was completed, the carrier flow was kept running for another two minutes to sweep the chamber clear of

fluorescent particles. The flow chamber was subsequently characterized using transmission bright field and epi-fluorescence microscopy. Three images were captured at the center of each well and the numbers of magnetic particles were counted in each image with the MetaVue (Downingtown, PA, USA) analysis software package and the numbers of fluorescent particles were counted manually. The total assay took 30–60 min, depending on the sample volume.

Results and discussion

Magnetophoretic separation

The performance of the MFS was characterized by measuring the distribution of magnetic and fluorescent particles in each collection well, using bright field and epi-fluorescence microscopy, respectively. Fig. 2 presents images acquired in the well located 25 mm from the first well in the flow chamber. The black regions in the bright field image, Fig. 2A, are characteristic of the magnetic particles, which appear to form networks that were either one or two particle layers thick. The magnetic particles strongly adsorb light due to their high Fe₃O₄ content and individual particles could be easily identified using a 40 \times objective. Fig. 2B presents an epi-fluorescence image, collected from the same region in Fig. 2A, in which individual fluorescent particles can be identified. Fig. 2C presents a higher resolution composite bright field and epi-fluorescence image of the lower right-hand region of Fig. 2A. Two observations can be made about the magnetophoretic separation process from these images. First, the number of magnetic particles in each well was significantly greater than the number of fluorescent particles. Second, although the magnetic particles strongly adsorb light across the whole visible spectrum, individual fluorescent particles could be easily identified in the epi-fluorescence images. Of the eleven fluorescent particles observed in the Fig. 2B, seven produced high-intensity images and four produced

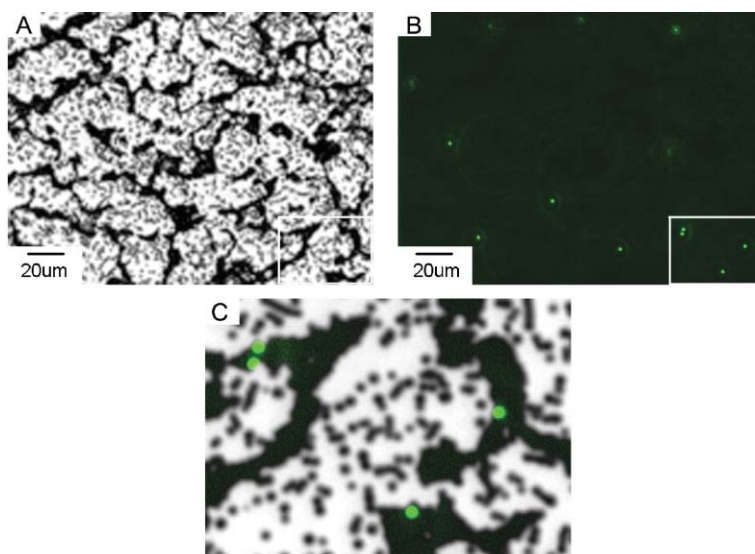


Fig. 2 Optical microscope images of the particles collected in the well 25 mm downstream from the particle inlet from a 5 ml sample of 100 PFU ml⁻¹. (A) Bright field microscope images collected with a 40 \times objective. (B) Epi-fluorescence microscope image collected with a 40 \times objective. The bright spots are fluorescent particles. (C) Composite bright field and epi-fluorescence image collected with a 40 \times objective.

low-intensity images. The high intensity particles appear to result from fluorescent-magnetic assemblies that are located in the plane of the magnetic particles. The low intensity image particles were found to be mobile, which suggested that they were not localized with the magnetic particles and thus were not associated with the virus. The attenuated intensity of these particles would result from the fact that the particles are located slightly above the image plane in which the magnetic particles reside. This difference in intensity was used to identify fluorescent-magnetic particle complexes.

Fig. 3 presents the results of the measurement of the number of fluorescent particles and coverage of magnetic particles in each well resulting from the magnetophoretic separation of a 100 PFU ml^{-1} sample. Three observations can be made about the results presented in Fig. 3. First, it appears that significantly more magnetic particles were collected in the wells from 0 to 25 mm than from 25 to 50 mm. A point that is not obvious from this figure is that the magnetic particles collected at a location that is significantly shorter than would be predicted for a single magnetic-fluorescent particle complex (we will revisit this fact in the Discussion section). Second, the peak in fluorescent particle collection takes place in the region between 5–25 mm and is shifted approximately 5 mm downstream from magnetic particle maximum. Third, approximately six fluorescent particles were measured in each of the images collected in the wells located in the 25 to 50 mm region. In the subsequent experiments, the dengue concentration was increased to concentrations as high as 10^4 PFU ml^{-1} but the density of fluorescent particles in the wells of the 25–50 mm region was found to remain constant. The fluorescent particles in this region were treated as background because their

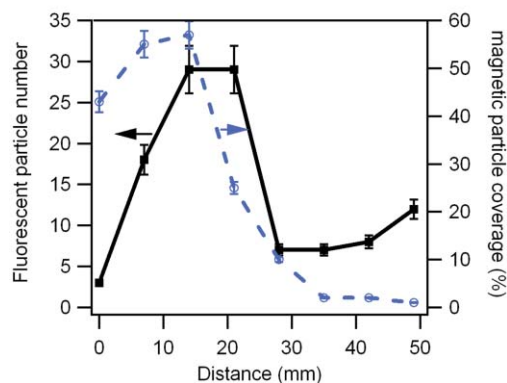


Fig. 3 Results of analysis of the number of fluorescent particles (■) and coverage of magnetic particles (○) measured in the collection wells along the separator at a dengue virus concentration of 100 PFU ml^{-1} in 5 ml. The distance scale in this figure is referenced to the first collection well. Only the high intensity fluorescent particles co-localized with the magnetic particles were counted in this measurement. The coverage of magnetic particles was determined by measuring the area of the black regions in each image. The standard deviation reported at each point was calculated by analyzing three separate regions in the central area of each well (regions outside of the center of the wells had very few magnetic microparticles as a result of the laminar flow conditions and 1 mm wide entrance region of the magnetic particles into the carrier fluid).

total density was found to be independent of the virus concentration.

Performance of the magnetophoretic fluorescence sensor

The performance of the MFS was assessed by characterizing the influence of reaction time, sample volume, and the presence of yellow fever virus on its background. The influence of reaction time on sensitivity was characterized by varying the incubation time of the reaction in which 1×10^4 magnetic particles ml^{-1} and 7×10^4 fluorescent particles ml^{-1} were reacted with 1000 PFU ml^{-1} virus in a 5 ml sample volume. Fig. 4 presents the total number of fluorescent particles measured across all wells as a function of incubation time. These results indicate that the number of fluorescent-magnetic particle assemblies formed was independent of incubation times greater than 5 min for dengue virus concentrations of 1000 PFU ml^{-1} . The rapid kinetics of this assay appears to result from the favourable mass transport conditions created by rapidly mixing of high densities of fluorescent and magnetic particles with the virus (this point will be addressed in the Discussion).

Fig. 5 presents the response of the MFS as a function of virus concentration and sample volume. The total number of fluorescent particles collected in all wells was measured as a function of dengue virus concentration and sample volumes using a 15 min reaction time. These results indicate that the detection threshold for the 5 and 20 ml sample volumes was 100 and 10 PFU ml^{-1} , respectively. The high sensitivity of the MFS appears to result from the favorable kinetics of the microparticle reaction, the efficiency of the separation of the fluorescent particles achieved by magnetic separation, and the fact that the particles are concentrated in a manner that made it possible to accurately determine the number of fluorescent particles co-localized with magnetic particles. The cross reactivity of the antibody was tested with yellow fever virus, a related flavivirus. In a control experiment, 10^4 PFU ml^{-1} of UV-inactivated yellow fever viruses were added to a serum sample. There was no detectable difference in the number of fluorescent particles separated from the yellow fever and the blank samples.

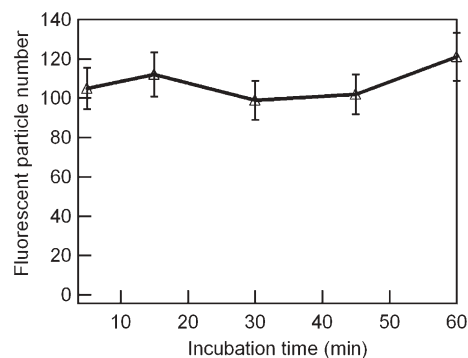


Fig. 4 The total number of fluorescent particles collected in the MFS at incubation times of 5, 15, 30, 45 and 60 min. The standard deviation was calculated from the variation in the sum of the particles measured at three points in each well. This measurement was made on 1000 PFU ml^{-1} in a 5 ml sample of 10% fetal calf serum.

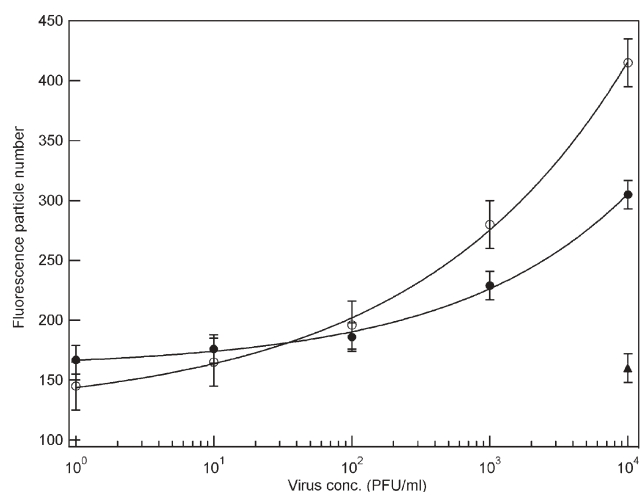


Fig. 5 Total numbers of the fluorescent particles measured in the MFS at various dengue virus concentrations for 5 ml (●) and 20 ml (○) reaction volume. The yellow fever detection (▲) was performed at 5 ml volume. The incubation time was 15 min. The standard deviation was calculated from the variation in the sum of the particles measured at three points in each well.

Magnetophoretic separation in concentrated suspensions

High gradient magnetophoretic separation is a technique that has been used to extract magnetic materials from complex mixtures.⁹ Magnetophoretic separation for bioanalytical means has recently been described at much lower flow rates.¹⁵ Two observations were made in this study that were not consistent with our expectations based on previous studies of magnetophoresis in dilute solutions. First, the fluorescent particles were collected in the wells located between 5–25 mm, rather than the later wells of the magnetophoretic separator. Second, a large number of magnetic particles were collected with the fluorescent particles in the wells. To understand these results we present a highly simplified theoretical framework for magnetophoresis.

In dilute solutions the performance of magnetophoretic separator can be analyzed in terms of the mobility of the magnetic particles and magnetic–fluorescent particle assemblies. The velocity at which a magnetic particle moves at steady state (v) is

$$v = \frac{F}{\zeta}, \quad (1)$$

where F is the magnetic force applied to the particle and ζ is the frictional resistance of the particle.²⁵ The force applied to a magnetic particle by an external magnetic field (B) is

$$F = M(B)V \frac{dB}{dy}, \quad (2)$$

where $M(B)$ is the volumetric magnetization of the magnetic particle, V is the volume of the particle, and dB/dy is the magnetic field gradient (the orientation of the axes is defined in Fig. 1).²⁶ Thus, the steady-state magnetic velocity (v_m) in a constant magnetic field gradient is determined by the balance

between the magnetic force (eqn (2)) and the drag force (eqn (1))

$$v_m = \frac{F}{\zeta} = \frac{2}{9\mu} \frac{r_m^3}{r_h} M \frac{dB}{dy} \quad (3)$$

where we have assumed the particle is spherical (*i.e.*, the drag is $6\pi\mu r_h$),²⁷ the viscosity μ of the solution is a constant, the hydrodynamic radius is r_h , and the magnetic radius is r_m . The average distance that the particles travel in the x -direction (x_{final}) may be estimated by assuming the velocity of the particles is constant in both x and y direction. This assumption is reasonable considering the rather narrow width of the flow chamber. This distance is proportional to the hydrodynamic radius of the assembly and inversely proportional to the cube of the magnetic particle radius

$$x_{\text{final}} = \bar{v}_h \frac{Y}{\bar{v}_m} \propto \frac{r_h}{r_m^3}, \quad (4)$$

where we have assumed the particles move in the flow chamber with a uniform velocities \bar{v}_h and \bar{v}_m in the x and y direction, respectively; and particles have a uniform initial velocity (\bar{v}_h) and position (y). Hence, assemblies that are different in hydrodynamic or magnetic size can be collected at different locations in a magnetophoretic sensor. Under the experimental conditions used in this study the magnetic field and magnetic field gradient above the center of the magnet are 2120 Gauss and 1050 Gauss cm^{-1} , respectively. This magnet produces a force of 0.55 pN on the superparamagnetic particles. In such conditions, the free magnetic and fluorescent–virus–magnetic particle assemblies should be collected at $x_{\text{final}} = 42$ and 53 mm from their entrance into the flow chamber, respectively. In this simplified analysis the variation in x_{final} only results from the variation in the radius of magnetic particles. Thus, the results presented in Fig. 3 do not appear to be consistent with dilute particle theory.

Insight into the mechanism of magnetophoretic separation in concentrated solutions was gained by studying superparamagnetic microparticles without flow. Fig. 6 presents bright field optical images of a suspension of magnetic particles as a magnetic field was applied (B–C) and removed (D) from the suspension. The assembly of superparamagnetic particles into linear chains in the presence of a magnetic field is a well known phenomenon that results from the strong magnetic forces between particles and the highly asymmetric fields produced by the chains in the external magnetic field. Chain formation will take place in ~ 2.7 s at the particle concentration of 5×10^4 particles ml^{-1} in a magnetic field of 980 Gauss based on the attractive magnetic force.²⁸ The velocity of the carrier fluid is 4.4 mm s^{-1} , thus chains of magnetic particles are expected to form approximately 11 mm into the separator. Once a chain forms, the magnetophoretic mobility becomes proportional to the number of particles in the chain as to the hydrodynamic drag of an ellipsoid is

$$\zeta = \frac{4\pi\mu r_{h,1}}{\ln(2r_{h,1}/r_{h,2}) - 1/2}, \quad (5)$$

where $r_{h,1}$ is the minor axis and $r_{h,2}$ is the major axis of the ellipsoid.²⁹ Chain assembly appears to account for the

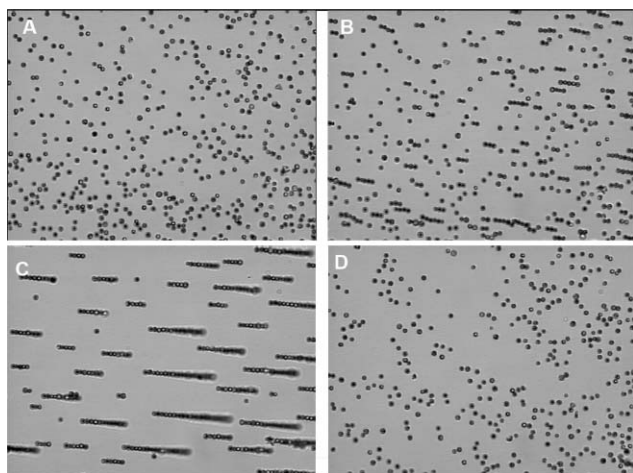


Fig. 6 Behavior of superparamagnetic microparticles in the presence of a magnetic field. (A) No magnetic field. (B) Magnetic field applied for less than 1 s. (C) Magnetic field applied for 2 s. (D) Magnetic field released for 4 s. The particle concentration was $\sim 5 \times 10^8$ particles ml^{-1} .

magnetophoretic separation behavior observed in this study. That is, the collection of a large fraction of the magnetic particles in the 0–25 mm wells is consistent with the assembly of approximately two superparamagnetic microparticles into a chain in the flow chamber. The 5 mm downstream shift of the fluorescent–magnetic particle assemblies was also consistent with the higher hydrodynamic drag of these structures.

Kinetics of the magnetophoretic fluorescence sensor

The response time and sensitivity for the MFS were determined by the kinetics of the reaction of the virus with the antibody functionalized magnetic and fluorescent particles to form magnetic–fluorescent particles assemblies. The relative importance of the diffusion, convection, and reaction rates in this process may be assessed using dimensional analysis. The three dimensionless groups that characterize the dominant mass transfer processes are: (1) the Reynolds number, which is $\frac{vr_h\rho}{\mu}$ where v is the velocity and ρ is the density of water;²⁵ (2) the Sherwood number, which is $\frac{hr_h}{D}$ where h is the convection coefficient and D is the diffusion coefficient;³⁰ and (3) the second Damkohler number, which is $\frac{k_{\text{on}}r_h^2}{D}$ where k_{on} is the on-rate of the reaction.³¹

Momentum transfer takes place in the creeping flow regime as the Reynolds number is $\sim 3 \times 10^{-5}$ (the average velocity of the particles in the reaction was $\sim 1 \text{ cm s}^{-1}$). The Sherwood number for creeping flow about a sphere is simply 2 and thus convection is the dominant form of mass transport.³⁰ The diffusion coefficient of the magnetic particle, fluorescent particle, and Dengue virus were calculated for the using the Einstein–Smoluchowski equation³² to be 4.4×10^{-9} , 4.4×10^{-9} and $7.3 \times 10^{-8} \text{ cm}^2 \text{ s}^{-1}$, respectively. The typical values of k_{on} and k_{off} for antibodies are between 10^3 – $10^4 \text{ M}^{-1} \text{ s}^{-1}$ and 10^{-2} – 10^{-4} s^{-1} , respectively.³³ Thus, the Damkohler number is much greater than 1 for the antibody concentrations used in this study,^{18,34} which necessarily means that the rate of

the chemical reaction is much greater than the rate of diffusion.

The image that emerges of the magnetic–fluorescent–virus reaction from dimensional analysis is that the rate of particle assembly was initially determined by the rate of convective transport of the virus to the particles. The relevant time scale for this process is $t = \frac{\langle x \rangle}{h}$, where $\langle x \rangle$ is the average distance between particles and h is the convection coefficient. The average convection coefficient for a sphere in the limit of very low Reynolds number is³⁵

$$h = \frac{D}{r_h} \quad (6)$$

The convection coefficient for the microparticles is $8.8 \times 10^{-6} \text{ cm s}^{-1}$. Thus, the time scale for the virus transport to the microparticle is 530 s (approximately 9 min) for a particle density of 10^4 per millilitre and this is the rate limiting step as the rate of reaction of the virus with the particle is much faster. The diffusion coefficient of the sphere under these conditions is three orders of magnitude higher than that of a flat surface, which is one of the primary reasons that MFS is significantly faster than solid phase immunoassays.

After the virus has reacted with a microparticle, the rate of the interparticle reaction will control the formation of magnetic–fluorescent particle complexes. This time scale will be determined by the hydrodynamic conditions of the mixture of particles and require complex numerical simulations to accurately define. However, the study of the reaction of dengue virus with the magnetic and fluorescent particles as a function of time indicated that the optimum condition was reached in less than 10 min for the 1000 PFU ml^{-1} sample. This suggests that the number of fluorescent–magnetic particle assemblies measured by the MFS was determined by the particle–particle reaction is quite fast. The binding constant of the monoclonal antibodies used in this study is anticipated to be in the 10–100 nM range. The reversibility of the virus–antibody bond could decrease the number of fluorescent–magnetic particle assemblies. However, recent observations suggest that the effective binding constant is much higher because the antibodies on the microparticles can bind to multiple epitopes on the virus.³⁶

Conclusions

In this report we have demonstrated magnetophoresis can be used to detect dengue type 2 virus at concentrations as low as 10 PFU ml^{-1} in 10% fetal calf serum. This sensitivity is 1000 times higher than that of a solid phase immunoassays for dengue and 100 times higher than flow cytometry assays for dengue.³⁷ Reaction times of only 15 min were found to be sufficient to achieve this sensitivity. We attribute the favorable sensitivity and reaction time of the sensor to the polyvalent binding of the antibody functionalized particle to the virus and the favorable kinetics associated with the reaction of high densities of magnetic and fluorescent particles. Magnetophoretic separation allows the fluorescent–magnetic particle complexes to be quickly identified with a high signal to noise ratio. A surprising observation was that magnetophoresis was dominated by the assembly of chains of magnetic

particles. Currently, magnetophoresis takes 40 min to perform on a 20 ml sample. Increasing the width of the entrance region of the magnetic particle into the carrier fluid should allow us to decrease the separation time to 2 min. An advantage of the MFS, which has not been described in this report, but is clear from the configuration of the assay, is that different color fluorescent particles may be used to simultaneously detect several pathogens. Two limitations of the assay are: (1) some fraction of the analyte will always be lost due to the formation of double fluorescent and magnetic particle assemblies that are not detected; and (2) higher order structures could form at higher concentrations of virus or when the size of the analyte approaches that of the particles.

Acknowledgements

This research has been funded by the NASA Institute for Nanoelectronics and Computing (NASA NCC 2-1363) to GUL and an National Institutes of Health award to RJK (P01 AI55672). We would also like to acknowledge the assistance we have received from Steven Wereley, Eric Born, and Michael Benko, in optimizing the design of the magnetophoretic separator. We thank John Roehrig (CDC, Fort Collins) for providing the 9A3D-8 hybridoma cell.

References

- D. M. Bell, *Emerging Infect. Dis.*, 2004, **10**, 1900–1906.
- B. Olsen, V. J. Munster, A. Wallensten, J. Waldenstrom, A. D. M. E. Osterhaus and R. A. M. Fouchier, *Science*, 2006, **312**, 384–388.
- D. van Riel, V. J. Munster, E. de Wit, G. F. Rimmelzwaan, R. A. M. Fouchier, A. D. M. E. Osterhaus and T. Kuiken, *Science*, 2006, **312**, 399–399.
- J. T. Kemshead, J. Ugelstad, A. Rembaum and F. Gibson, *Eur. J. Cancer Clin. Oncol.*, 1982, **18**, 1043–1043.
- J. G. Treleaven, F. M. Gibson, J. Ugelstad, A. Rembaum, T. Philip, G. D. Caine and J. T. Kemshead, *Lancet*, 1984, **1**, 70–73.
- A. Heeboll-Nielsen, S. F. L. Justesen, T. J. Hobbly and O. R. T. Thomas, *Sep. Sci. Technol.*, 2004, **39**, 2891–2914.
- G. P. Hatch and R. E. Stelter, *J. Magn. Magn. Mater.*, 2001, **225**, 262–276.
- M. C. Cheung, J. D. Goldberg and Y. W. Kan, *Nat. Gen.*, 1996, **14**, 264–268.
- Y. A. Liu and M. J. Cak, *AICHE J.*, 1983, **29**, 771–119.
- Y. A. Liu and M. J. Oak, *AICHE J.*, 1983, **29**, 780–789.
- S. C. Trindade, *Studies of the Magnetic Demineralization of Coal*, Massachusetts Institute of Technology, Cambridge, 1973.
- M. Zborowski, Y. Jing, L. R. Moore, P. S. Williams, S. Farag, B. Bolwell and J. J. Chalmers, *Exp. Hematol.*, 2007, **35**, 92–93.
- M. Zborowski, L. P. Sun, L. R. Moore, P. S. Williams and J. J. Chalmers, *J. Magn. Magn. Mater.*, 1999, **194**, 224–230.
- N. Pamme and C. Wilhelm, *Lab Chip*, 2006, **6**, 974–980.
- N. Pamme and A. Manz, *Anal. Chem.*, 2004, **76**, 7250–7256.
- K. H. Han and A. B. Frazier, *J. Appl. Phys.*, 2004, **96**, 5797–5802.
- G. N. Malavige, S. Fernando, D. J. Fernando and S. L. Seneviratne, *Postgrad. Med. J.*, 2004, **80**, 588–601.
- H. Shang, P. M. Kirkham, T. M. Myers, G. H. Cassell and G. U. Lee, *J. Magn. Magn. Mater.*, 2005, **293**, 382–388.
- H. Shang, W. S. Chang, S. H. Kan, S. A. Majetich and G. U. Lee, *Langmuir*, 2006, **22**, 2516–2522.
- Y. S. Hahn, R. Galler, T. Hunkapiller, J. M. Dalrymple, J. H. Strauss and E. G. Strauss, *Virology*, 1988, **162**, 167–180.
- R. J. Kuhn, W. Zhang, M. G. Rossmann, S. V. Pletnev, J. Corver, E. Lenches, C. T. Jones, S. Mukhopadhyay, P. R. Chipman, E. G. Strauss, T. S. Baker and J. H. Strauss, *Cell*, 2002, **108**, 717–725.
- P. J. Bredenbeek, E. A. Kooi, B. Lindenbach, N. Huijman, C. M. Rice and W. J. M. Spaan, *J. Gen. Virol.*, 2003, **84**, 1261–1268.
- J. T. Roehrig, R. A. Bolin and R. G. Kelly, *Virology*, 1998, **246**, 317–328.
- G. U. Lee, S. Metzger, M. Natesan, C. Yanavich and Y. F. Dufrene, *Anal. Biochem.*, 2000, **287**, 261–271.
- G. K. Batchelor, *An introduction to fluid dynamics*. U.P., Cambridge, 1967, 615 pp.
- D. Jiles, *Introduction to magnetism and magnetic materials*, 1st edn, Chapman and Hall, London, New York, 1991, 440 pp.
- F. M. White, *Viscous fluid flow*, 3rd edn, McGraw–Hill Higher Education, New York, NY, 2006, 629 pp.
- M. Widom and H. Zhang, *Phys. Rev. Lett.*, 1995, **74**, 2616–2616.
- F. Perrin, *J. Phys. Radium*, 1934, **7**, 497–511.
- T. K. Sherwood, R. L. Pigford and C. R. Wilke, *Mass transfer*, McGraw–Hill, New York, 1975, 677 pp.
- E. L. Cussler, *Diffusion : mass transfer in fluid systems*, 2nd edn, Cambridge University Press, New York, 1997, 580 pp.
- A. Einstein, *Investigations on the theory of the Brownian movement*, Dover Publications, New York, 1956, 119 pp.
- C. R. Cantor and P. R. Schimmel, *The behavior of biological macromolecules*, W. H. Freeman, San Francisco, 1980, 624 pp.
- S. W. Metzger, M. Natesan, C. Yanavich, J. Schneider and G. U. Lee, *J. Vac. Sci. Technol., A*, 1999, **17**, 2623–2628.
- S. Whitaker, *AICHE J.*, 1972, **18**, 361–371.
- J. Baudry, C. Rouzeau, C. Goubault, C. Robic, L. Cohen-Tannoudji, A. Koenig, E. Bertrand and J. Bibette, *Proc. Natl. Acad. Sci. U. S. A.*, 2006, **103**, 16076–16078.
- C. R. Lambeth, L. J. White, R. E. Johnston and A. M. de Silva, *J. Clin. Microbiol.*, 2005, **43**, 3267–3272.